

Motion Detecting Artificial Retina Model by Two-Dimensional Multi-Layered Analog Electronic Circuits

Masashi KAWAGUCHI^{†,††a)}, *Student Member*, Takashi JIMBO^{††},
and Masayoshi UMENO^{†††}, *Regular Members*

SUMMARY We propose herein a motion detection artificial vision model which uses analog electronic circuits. The proposed model is comprised of four layers. The first layer is a differentiation circuit of the large CR coefficient, and the second layer is a differentiation circuit of the small CR coefficient. Thus, the speed of the movement object is detected. The third layer is a difference circuit for detecting the movement direction, and the fourth layer is a multiple circuit for detecting pure motion output. When the object moves from left to right the model outputs a positive signal, and when the object moves from right to left the model outputs a negative signal. We first designed a one-dimensional model, which we later enhanced to obtain a two-dimensional model. The model was shown to be capable of detecting a movement object in the image. Using analog electronic circuits, the number of connections decrease and real-time processing becomes feasible. In addition, the proposed model offers excellent fault tolerance. Moreover, the proposed model can be used to detect two or more objects, which is advantageous for detection in an environment in which several objects are moving in multiple directions simultaneously. Thus, the proposed model allows practical, cheap movement sensors to be realized for applications such as the measurement of road traffic volume or counting the number of pedestrians in an area. From a technological viewpoint, the proposed model facilitates clarification of the mechanism of the biomedical vision system, which should enable design and simulation by an analog electric circuit for detecting the movement and speed of objects.

key words: *neural network, motion detection, analog circuits, artificial retina, two-dimensional circuits*

1. Introduction

We propose herein a motion detection artificial vision model using analog electronic circuits. A neuro chip and an artificial retina chip are developed to comprise the neural network model and simulate the biomedical vision system. At present, basic image processing,

such as edge detection and reverse display of an image has been achieved [1], [2]. In the present study, we develop a motion detection model using an analog electronic circuit. We measured the shape of the output waves produced by the input movement signal using an electronic circuit simulator (SPICE). The retina is composed of visual cells, horizontal cells, bipolar cells, amacrine cells, and ganglion cells. Amacrine cells are thought to receive input from bipolar cells over a wide area through excited synapses, and time and spatial changes have been detected in the output of bipolar cells. Therefore, the amacrine cell is able to recognize the movement object in the biomedical vision system. In the retina, not only is an optical signal converted into a nerve impulse, but also the complex signal is processed. The signal is then sent to the brain through the retina. Thus, in the biomedical system, the retina functions as a sensor for the image input.

The retina consists of the inside retina and outside retina. The inside retina sends the nerve impulses to the brain, whereas the outside retina receives optical input from the visual cell. As a result, the outside retina emphasizes spatial changes in optical strength. Recently, the network between the amacrine cell, the bipolar cell and the ganglion cell has been clarified theoretically, which has led to active research concerning the neuro device, which models the structure and function of the retina. Easy image processing, reversing, edge detection, and feature detection, have been achieved by technologies such as the neuro chip and the analog VLSI circuit. Some motion detection models are proposed in the recent research. One paper describes the application of an analog VLSI vision sensor to active binocular tracking. The sensor outputs are used to control the vergence angles of the two cameras and the tilt angle of the head so that the center pixels of the sensor arrays image the same point in the environment [3]. Another model is presented the implementation of a visual motion detection algorithm on an analog network. The algorithm is on Markov random field(MRF) modeling. Robust motion detection is achieved by using a spatiotemporal neighborhood for modeling pixel interactions. Not only are the moving edges detected, but also the inner part of moving re-

Manuscript received June 22, 2002.

Manuscript revised September 8, 2002.

Final manuscript received October 23, 2002.

[†]The author is with the Department of Electrical Engineering, Suzuka National College of Technology, Suzuka-shi, 510-0294 Japan.

^{††}The authors are with the Department of Environmental Technology and Urban Planning Graduate School of Engineering, Nagoya Institute of Technology, Nagoya-shi, 466-8555 Japan.

^{†††}The author is with the Department of Electronic Engineering, Chubu University, Kasugai-shi, 487-8501 Japan.

a) E-mail: masashi@elec.suzuka-ct.ac.jp

gions [4]. The other model is an analog MOS circuit inspired by an inner retina. The analog circuit produces signals of motion of edges which are output in an outer retinal neural network. Edge signals are formed into half-wave rectified impulses in 2 types of amacrine cells, and fed back to the wide field amacrine cell in order to modulate width of impulses [5].

In the present study, we propose a motion detection model in which the speed is detected by differentiation circuits. The surface layer is composed of the connections of capacitors. In the inner layer, the movement direction is detected by difference circuits. When the object moves from left to right, a positive output signal is generated, and when the object moves from right to left, a negative output signal is generated. We show this model is able to detect the speed and direction of a movement object by the simple circuits. Despite the large object size, this model can detect the motion. The connection of this model is between adjacent elements, making hardware implementation easy.

2. One-Dimensional Model

We first composed a one-dimensional model, the structure of which is shown in Fig. 1.

The characteristic of this model is realized by two capacitors placed in series in the input layer. As a

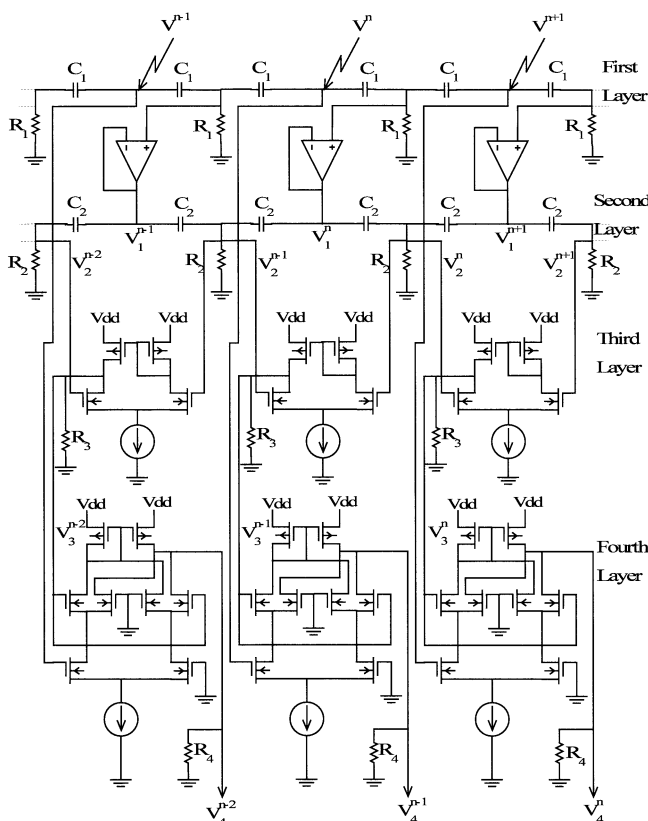


Fig. 1 One-dimensional four-layer motion detection model.

result, the input signal does not transmit output directly. Only a pure differentiation element is allowed to transmit to the next layer. The surface layer is a differentiation circuit realized by CR. The object speed is detected by the differentiation circuit, and the direction of the movement is detected by the difference circuit. The CR circuit of the surface layer corresponds to the visual cell of the retina cell, and the MOSFET differentiation circuit corresponds to the amacrine cell which detects movement information in the retina [6], [7].

2.1 First Layer Differentiation Circuits (First Layer)

The current is given by Eq. (1), where the input voltage is denoted by V^n and the capacitance is denoted by C_1 . The current into a capacitor is the derivative with respect to time of the voltage across the capacitor, multiplied by the capacitance. The output voltage V_1^n is given by Eq. (2). Equation (2) is multiplied the resistance R_1 , calculating the voltage potential.

$$I = C_1 \frac{dV^n}{dt} \quad (1)$$

$$V_1^n = IR_1 = C_1 R_1 \frac{dV^n}{dt} \quad (2)$$

Buffer circuits are realized by operational amplifiers between the first layer and the second layer.

2.2 Second Layer Differentiation Circuits (Second Layer)

The second Layer is also composed of differentiation circuits; however, the CR coefficient is small compared that of the first layer differentiation circuits. The output of first layer, V_1^n , is differentiated again, and the output of the second layer is assumed to be V_2^n , calculating the voltage potential.

$$I = C_2 \frac{dV_1^n}{dt} \quad (3)$$

$$V_2^n = IR_2 = C_2 R_2 \frac{dV_1^n}{dt} \quad (4)$$

2.3 Difference Circuits (Third Layer)

The third layer consists of difference circuits realized by MOSFET. In Fig. 2, the bottom I_b is a current source. The manner in which I_b is divided between Q_1 and Q_2 is a sensitive function of the difference between V_2^{n+1} and V_2^n , and is the essence of the operation of the stage. We assume the MOSFET device is in the sub-threshold region, the I - V characteristics follows the exponential characteristics, then the drain current I_D in the sub-threshold region is exponential in the gate voltage V_g and source voltage V_s . V is electric potential of current

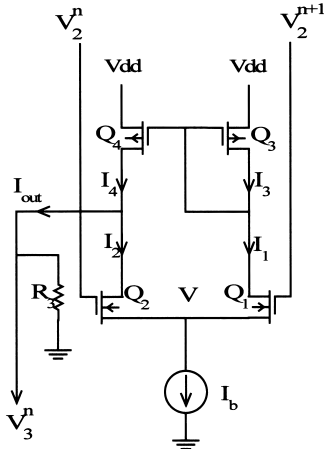


Fig. 2 Difference circuits (third layer).

source I_b . I_0 and κ are coefficients.

$$I_D = I_{sat} e^{\kappa V_g - V_s} \quad (5)$$

Applying this expression to Q_1 and Q_2 , we obtain

$$I_1 = I_0 e^{\kappa V_2^{n+1} - V} \quad \text{and} \quad I_2 = I_0 e^{\kappa V_2^n - V} \quad (6)$$

The sum of the two drain currents must be equal to I_b :

$$I_b = I_1 + I_2 = I_0 e^{-V} \left(e^{\kappa V_2^{n+1}} + e^{\kappa V_2^n} \right) \quad (7)$$

We can solve this equation for the voltage V :

$$e^{-V} = \frac{I_b}{I_0} \frac{1}{e^{\kappa V_2^{n+1}} + e^{\kappa V_2^n}} \quad (8)$$

Substituting Eq. (8) into Eq. (6), we obtain expression for the two drain currents:

$$I_1 = I_b \frac{e^{\kappa V_2^{n+1}}}{e^{\kappa V_2^{n+1}} + e^{\kappa V_2^n}} \quad \text{and} \quad I_2 = I_b \frac{e^{\kappa V_2^n}}{e^{\kappa V_2^{n+1}} + e^{\kappa V_2^n}} \quad (9)$$

This difference is

$$I_1 - I_2 = I_b \frac{e^{\kappa V_2^{n+1}} - e^{\kappa V_2^n}}{e^{\kappa V_2^{n+1}} + e^{\kappa V_2^n}} \quad (10)$$

Multiplying both the numerator and denominator of Eq. (10) by $e^{-(V_2^{n+1} + V_2^n)/2}$, we can express every exponent in terms of voltage differences. The result is

$$\begin{aligned} I_1 - I_2 &= I_b \frac{e^{\kappa(V_2^{n+1} - V_2^n)/2} - e^{-\kappa(V_2^{n+1} - V_2^n)/2}}{e^{\kappa(V_2^{n+1} - V_2^n)/2} + e^{-\kappa(V_2^{n+1} - V_2^n)/2}} \\ &= I_b \tanh \frac{\kappa(V_2^{n+1} - V_2^n)}{2} \end{aligned} \quad (11)$$

The circuit consists of a differential pair and a single current mirror, like the one shown in Fig. 2, which is used to subtract the drain currents I_1 and I_2 . The current I_1 drawn out of Q_3 is reflected as an equal current out of Q_4 ; the output current I_{out} is thus equal to $I_1 - I_2$, and is therefore given by Eq. (11).

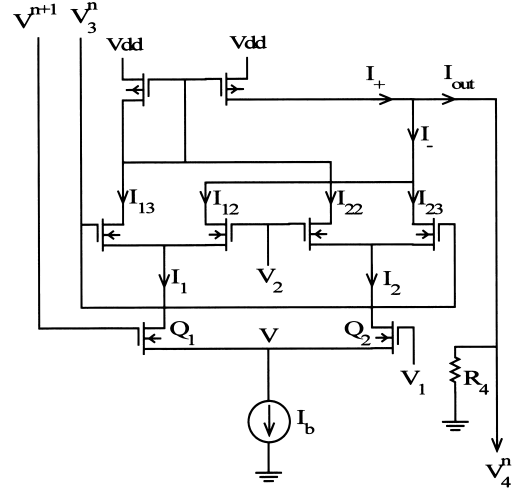


Fig. 3 Gilbert multiple circuits (fourth layer).

The output voltage of this circuit is as follows.

$$\begin{aligned} V_3^n &= (I_1 - I_2) R_3 \\ &= I_b R_3 \tanh \frac{\kappa(V_2^{n+1} - V_2^n)}{2} \end{aligned} \quad (12)$$

Using the difference circuits, we obtain the peak output value of movement. V_2^n and V_2^{n+1} are the second layer outputs of the neighbor terminal, V_3^n is the third layer output. R_3 is the earth resistance.

2.4 Gilbert Multiple Circuits (Fourth Layer)

The fourth layer is comprised of Gilbert multiple circuits. We show it in Fig. 3. We assume the MOSFET device is in the sub-threshold region, the I - V characteristics follows the exponential characteristics, then the drain current I_D in the sub-threshold region is exponential in the gate voltage V_g and source voltage V_s . The result for the two drain currents of the differential pair were derived in Eq. (9).

$$\begin{aligned} I_1 &= I_b \frac{e^{\kappa V^{n+1}}}{e^{\kappa V^{n+1}} + e^{\kappa V_1}} \\ &= \frac{I_b}{2} \left(1 + \tanh \frac{\kappa(V^{n+1} - V_1)}{2} \right) \end{aligned} \quad (13)$$

and

$$\begin{aligned} I_2 &= I_b \frac{e^{\kappa V_1}}{e^{\kappa V^{n+1}} + e^{\kappa V_1}} \\ &= \frac{I_b}{2} \left(1 - \tanh \frac{\kappa(V^{n+1} - V_1)}{2} \right) \end{aligned} \quad (14)$$

Similar reasoning applied to the two upper differential pairs fed by I_1 and I_2 leads to expressions for the four upper drain currents.

$$I_{13} = \frac{I_1}{2} \left(1 + \tanh \frac{\kappa(V_3^n - V_2)}{2} \right) \quad (15)$$

$$I_{12} = \frac{I_1}{2} \left(1 - \tanh \frac{\kappa(V_3^n - V_2)}{2} \right) \quad (16)$$

$$I_{23} = \frac{I_2}{2} \left(1 + \tanh \frac{\kappa(V_3^n - V_2)}{2} \right) \quad (17)$$

$$I_{22} = \frac{I_2}{2} \left(1 - \tanh \frac{\kappa(V_3^n - V_2)}{2} \right) \quad (18)$$

We sum I_{13} and I_{22} to create I_+ , the positive contribution to the output current. We can compute I_+ by adding Eqs. (15) and (18).

$$I_+ = \frac{I_1 + I_2}{2} + \frac{I_1 - I_2}{2} \tanh \frac{\kappa(V_3^n - V_2)}{2} \quad (19)$$

Similarly, I_{12} and I_{23} are summed to create I_- , the negative contribution to the output current. We can compare I_- by adding Eqs. (16) and (17).

$$I_- = \frac{I_1 + I_2}{2} - \frac{I_1 - I_2}{2} \tanh \frac{\kappa(V_3^n - V_2)}{2} \quad (20)$$

The output is formed by subtracting I_- from I_+ . We can thus compare I_{out} by subtracting Eq. (20) from Eq. (19).

$$I_{out} = (I_1 - I_2) \tanh \frac{\kappa(V_3^n - V_2)}{2} \quad (21)$$

Substituting Eqs. (13) and (14), we obtain:

$$I_{out} = I_b \tanh \frac{\kappa(V^{n+1} - V_1)}{2} \tanh \frac{\kappa(V_3^n - V_2)}{2} \quad (22)$$

In Fig. 1, V_1 and V_2 are connected to ground respectively. In this circuit, the voltage V_1 and V_2 are 0. The fourth layer produces the third layer output V_3^n and the input signal V^{n+1} . This circuit detects the pure output of movement. I_b is the current source, and κ is a coefficient [1].

$$I_4^n = I_b \tanh \frac{\kappa V_3^n}{2} \tanh \frac{\kappa V^{n+1}}{2} \quad (23)$$

$$V_4^n = I_4^n R_4 = I_b R_4 \tanh \frac{\kappa V_3^n}{2} \tanh \frac{\kappa V^{n+1}}{2} \quad (24)$$

I_4^n is the output current of the fourth layer, R_4 is the earth resistance, and V_4^n is the final output. I_4^n corresponds to I_{out} in Fig. 3.

Figure 4 shows the input and output signal of each layer. The output of the first layer indicates that input signal is differentiated by a large CR coefficient. The output of the second layer shows that the first layer output signal is differentiated by a small CR coefficient. V^{n+1} indicates the neighbor terminal of V^n . Therefore, the input signal of V^{n+1} is delayed compared to V^n . The difference between the second layer output V^{n+1} and V^n is calculated. The third layer output shows the peak positive signal. Finally, the fourth layer produces the third layer output V_3^n and the input signal V^{n+1} . This circuit detects the pure output of movement.

Figure 5 shows the input and output signal of each

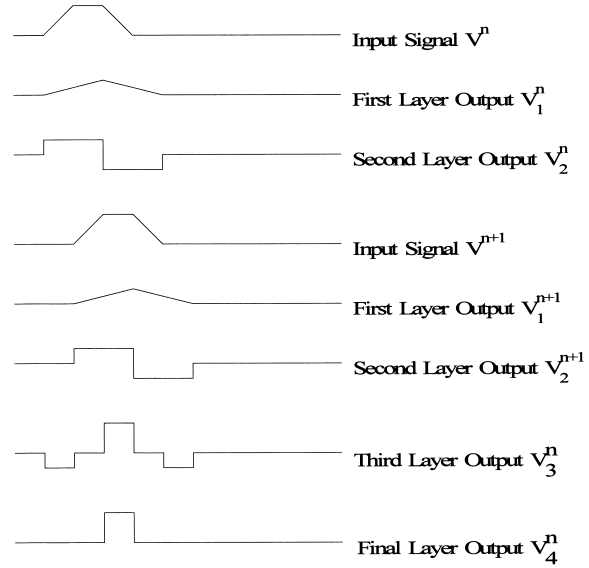


Fig. 4 Diagram of each layer and each terminal.

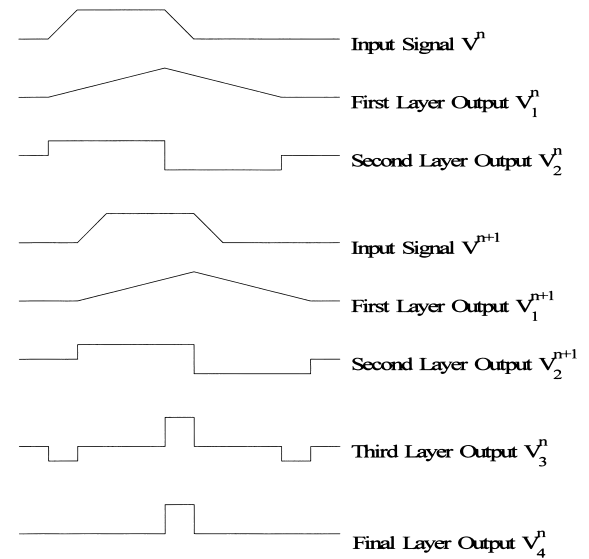


Fig. 5 Diagram of each layer and each terminal when the object size is large.

layer and each terminal when the object size is large. Despite the large object size, we obtain the peak signal of final output. Therefore, the proposed model can detect the moving object and is not affected by object size.

Figure 6 shows the shape of the moving object. When the object moves from left to right, the voltage will be input to each terminal as shown in Fig. 7. Figure 8 shows the output of the first layer, first-layer differentiation circuits. Figure 9 shows the output of the second layer, second-layer differentiation circuits. By using two layers of differentiation circuits, speed detection via the proposed model is not affected by object size.

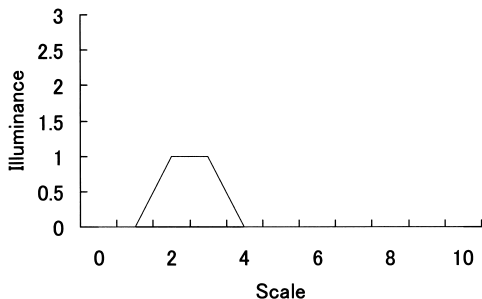


Fig. 6 Shape of a moving object.

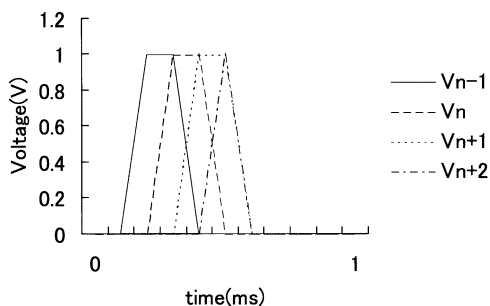


Fig. 7 Input voltage of each terminal.

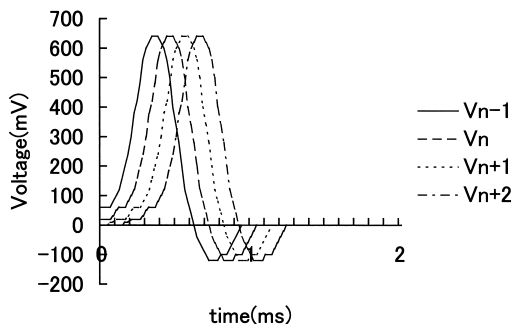


Fig. 8 Output of the first layer.

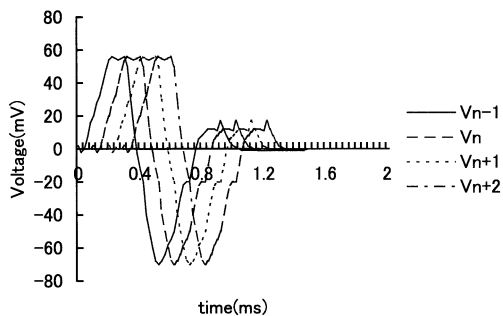


Fig. 9 Output of the second layer.

Figure 10 shows the output of the third-layer difference circuits. Figure 11 shows the final output, which indicates that this circuit detects the pure output of the movement. Figure 12 shows the final output when the object moves at half speed. Figure 13 shows the final output when the object moves from right to left.

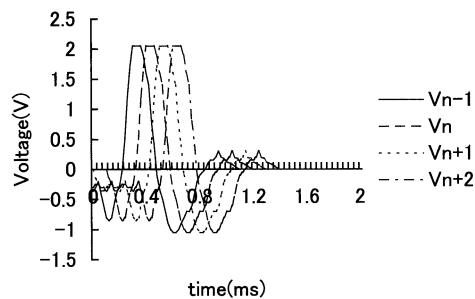


Fig. 10 Output of the third layer (after difference circuit processing).

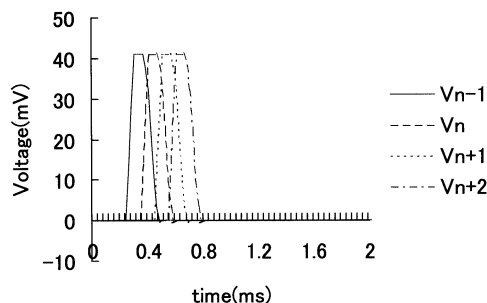


Fig. 11 Output of the fourth layer (after multiple circuit processing).

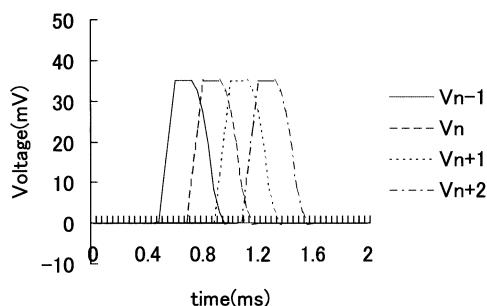


Fig. 12 Output of the half speed of input.

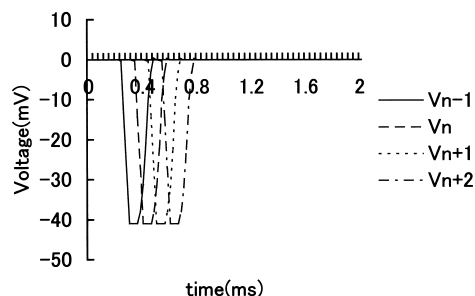


Fig. 13 Output of the reverse input direction.

When the object moves from right to left, this model outputs a negative signal. Figure 14 shows the final output when the object size is large, which is nearly identical to the result shown in Fig. 11, indicating that this model is not affected by object size, with respect to

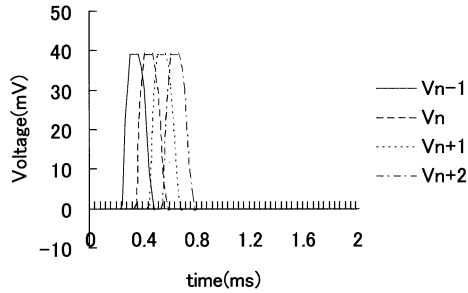


Fig. 14 Output when the object size is large.

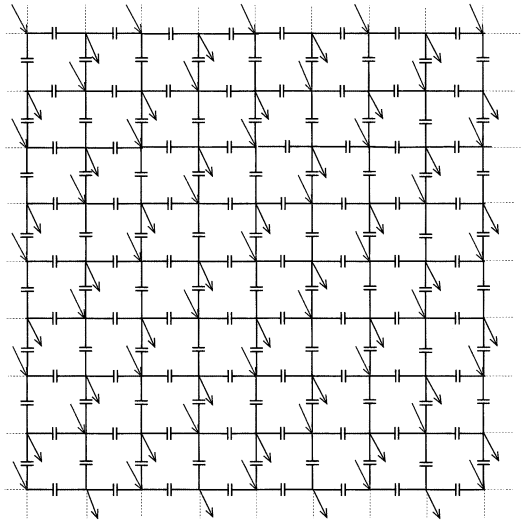


Fig. 15 Surface layer of the two-dimensional model.

speed detection. These results show that this model is able to detect the speed and direction of a movement object in one dimension. We set the parameter of circuits as follows. In the first layer, $C_1 = 0.1 \mu\text{F}$, $R_1 = 1 \text{ k}\Omega$. We used the $\mu\text{A}741$ as a buffer circuit. In the second layer, $C_2 = 0.1 \mu\text{F}$, $R_2 = 100 \text{ k}\Omega$. At the difference circuits, we used the VP1310 and VN1310 as MOSFET.

3. The Two-Dimensional Model

We enhanced the one-dimensional model to obtain a two-dimensional model. The first layer (surface layer) is an array of capacitors, similar to a lattice, which has a simple structure and allows easy differentiation. The first layer is shown in Fig. 15.

The second layer is also an array of capacitors similar to a lattice. The third layer consists of a subtraction circuit realized via a MOSFET. The input terminal and the output terminal of the first layer are arranged in alternating fashion. The proposed model differentiates the first and second layers, and the speed of the moving object is detected [8], [9]. The structure of the two-dimensional model is shown in Fig. 16. Figure 17 shows the shape of the moving object detected by the

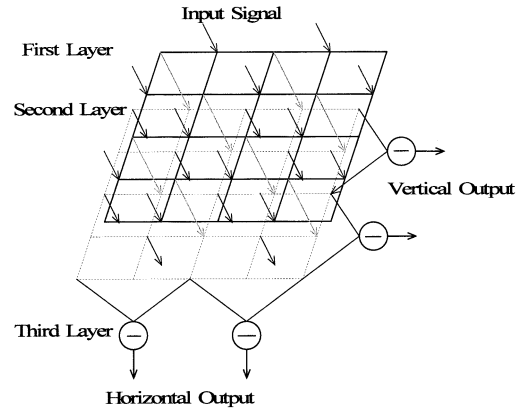


Fig. 16 Structure of the two-dimensional model.

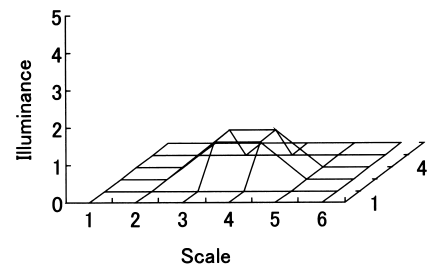
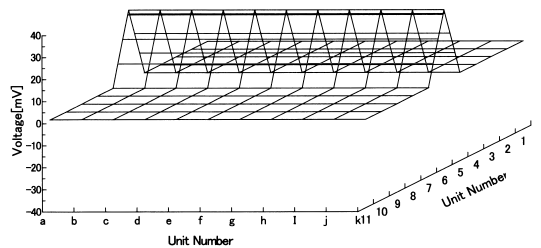


Fig. 17 Shape of moving object detected by the two-dimensional model.

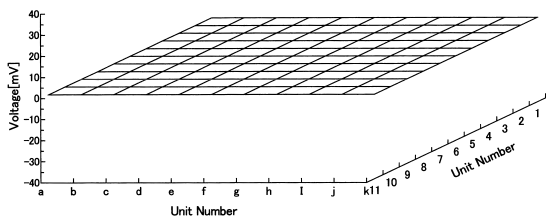
two-dimensional model.

The width of the brightness was assumed to be one pixel, and the width of the peripheral obscure part was assumed to be one pixel. In the two-dimensional model, we investigated six different conditions, and the horizontal outputs and the vertical outputs of each input are shown in Figs. 18 through 23. The inputs for the object movement are as follows: left to right, bottom to top, upper-right to lower-left, left to right changing speed from 1 to 1/2, and changing direction from right-to-left to upper-to-under and two objects moving simultaneously: one object is moving from left to right and the other object is moving from bottom to up.

In Fig. 18, because the output of a horizontal element is positive, a light source moving from left to right has been detected. Moreover, no vertical direction element was present and no movement in the vertical direction was detected. In contrast, no horizontal element is seen in Fig. 19. The output value of the vertical direction element is 1/2 compared to that of the horizontal element of Fig. 18, and the sign is negative. In Fig. 20, a horizontal element is indicated by the negative value and a vertical element is indicated by the positive value, indicating that diagonal movement from upper-right to lower-left has been detected. From these two-dimensional results, the speed of the movement object can be determined by the output value, and the direction of the movement object can be determined by the sign of the output value.

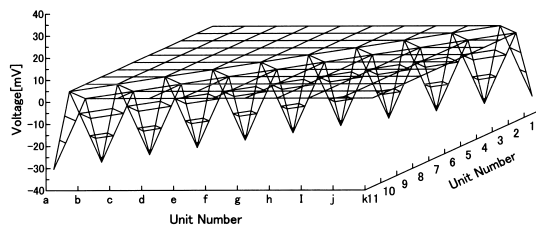


(a)

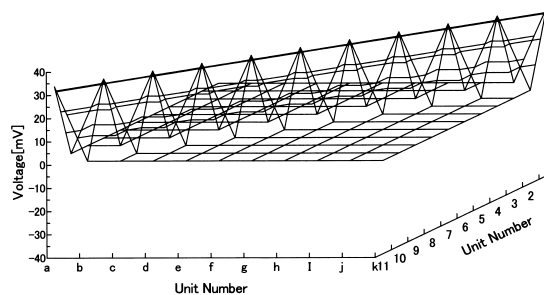


(b)

Fig. 18 (a) Horizontal output when the object moves from left to right. (b) Vertical output when the object moves from left to right.

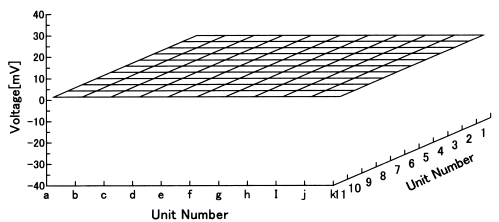


(a)

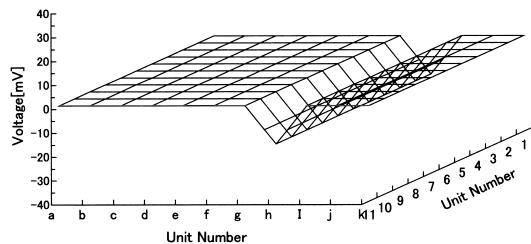


(b)

Fig. 20 (a) Horizontal output when the object moves from top-right to bottom-left. (b) Vertical output when the object moves from top-right to bottom-left.

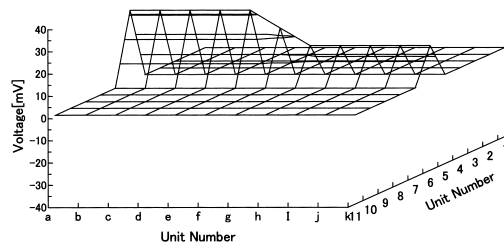


(a)

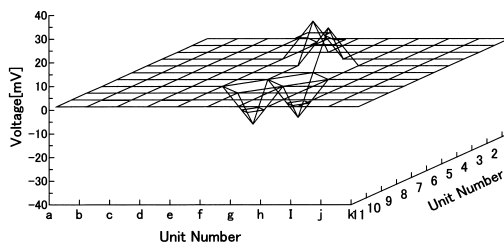


(b)

Fig. 19 (a) Horizontal output when the object moves from bottom to top at half speed. (b) Vertical output when the object moves from bottom to top at half speed.



(a)



(b)

Fig. 21 (a) Horizontal output when the object moves from left to right while varying the speed from 1 to 1/2. (b) Vertical output when the object moves from left to right while varying the speed from 1 to 1/2.

Figure 21 is the output when the object moves from left to right changing speed from 1 to 1/2. The output is shown to decrease along the way. Figure 22 is the horizontal output when the direction of the movement object changes from right-to-left to top-to-bottom. The results of Fig. 21 and Fig. 22 show that although the speed and direction of the movement object change, the output has been generated accordingly. In Fig. 23, the movement of two objects is output simultaneously. In Fig. 21 and Fig. 22, when the speed or direction is converted, or in Fig. 23, in the vicinity of the intersection of two movement objects, an extra output has

been generated. However, if the scale of the model is enhanced comprehensively, this will not present a significant problem.

These results indicate that detecting a moving object is possible when the direction of the movement object changes or when two or more objects move simultaneously. Moreover, no time delay exists between the input signal and the output signal, as is the case for one dimension. Thus, the two-dimensional model is

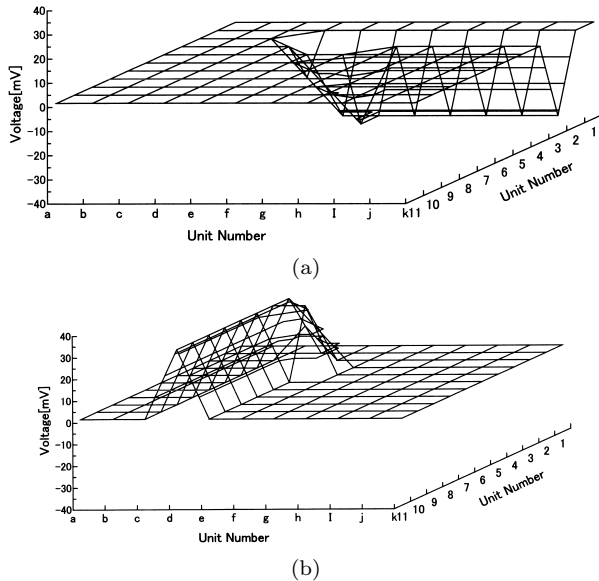


Fig. 22 (a) Horizontal output when the direction of movement of the object is changed from right-to-left to top-to-bottom. (b) Vertical output when the direction of movement of the object is changed from right-to-left to top-to-bottom.

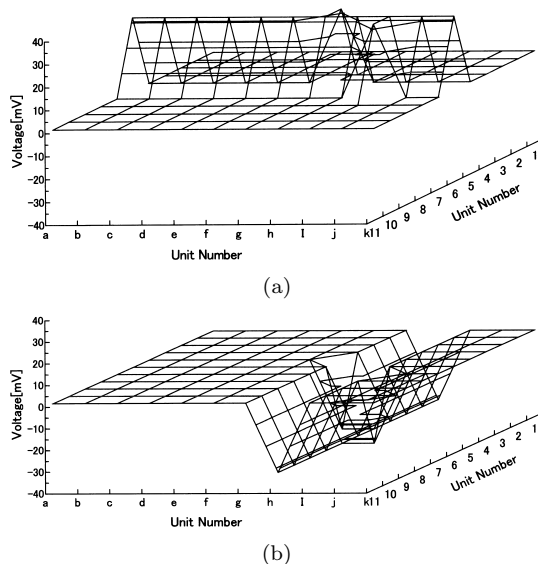


Fig. 23 (a) Horizontal output for two objects moving simultaneously: one object is moving from left to right and the other object is moving from bottom to top. (b) Vertical output for two objects moving simultaneously: one object is moving from left to right and the other object is moving from bottom to top.

able to detect the speed and the direction of the movement object in both one and two dimensions. Moreover, the output of the vertical direction can be deleted by adding a threshold circuit to each output terminal. As a result, element detection of the pure direction of the movement can be performed. In addition, detection of oblique movements is possible by integrating the vertical and horizontal directions of the movement.

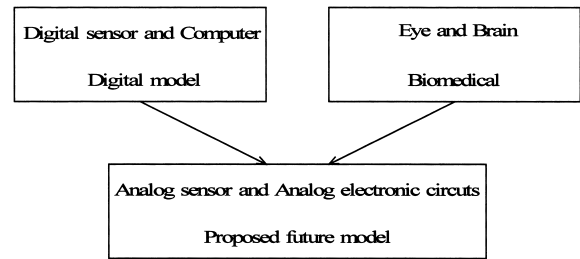


Fig. 24 Brain system using an analog electronic circuit.

4. Hardware Implementation

The proposed model is processed by analog electronic circuits. In the biomedical brain, information is also processed in an analog manner. In the future, movement information will be collected into an analog electronic brain model. This would allow the hardware system of the biomedical brain model to be realized. The proposed moving detection model has possible application as a sensor and can compose part of the receptor. The proposed model will enable the clarification of the mechanism of the biomedical brain. The present study attempts to realize a brain system using an analog electronic circuit, as described in Fig. 24.

5. Conclusion

We designed the motion detection analogue electric circuit using a biomedical vision system. We first designed the one-dimensional model and experimented. Using the one-dimension model, the movement information was detected. Next, we designed the two-dimensional model. The capacitor in the surface layer was arranged in a similar manner to the lattice in the two-dimension model. The input terminal and the output terminal were arranged in an alternating manner. As a result, a simple circuit and an equivalent output result were obtained. The realization of an integration device will enable the number of elements to be reduced. The proposed model is robust with respect to fault tolerance. Moreover, the connection of this model is between adjacent elements, making hardware implementation easy.

The proposed model is applicable to movement sensors, measurement of road traffic volume, speed measurement, and counting the number of pedestrians in an area. In addition, the proposed model may be applied in sensors for use in industrial or domestic products. Using the analog circuit not only simplifies the structure, but also provides excellent fault tolerance, as compared to digital circuits. Using the proposed model, moving objects can be detected even if two or more objects are present. This is advantageous for detection in environments in which several objects are moving in multiple directions simultaneously. Under these circumstances, previous scanning methods may lose sight

of the movement object. In the proposed model, since the motion is separately detected along the x and y axes, the movement information can be used as a vector.

The following problems will be examined in a future study. Simplification of the difference circuit and reduction of the number of connections is necessary in order to analyze input by devices such as CCDs. In addition, it needs the preprocessing circuits before input layer. Finally, this model attempts to aid in the clarification of the biomedical vision system, particularly the mechanism of motion recognition. From a technological viewpoint, the proposed model facilitates clarification of the mechanism of the biomedical vision system, which should enable design and simulation by an analog electric circuit for detecting the movement and speed of objects.

Acknowledgments

The present research was supported by the Okasan-Kato Foundation.

References

- [1] C. Mead, *Analog VLSI and Neural Systems*, Addison Wesley, 1989.
- [2] C.P. Chong, C.A.T. Salama, and K.C. Smith, "Image-motion detection using analog VLSI," *IEEE J. Solid-State Circuits*, vol.27, no.1, pp.93–96, 1992.
- [3] Z. Lu and B.E. Shi, "Subpixel resolution binocular visual tracking using analog VLSI vision sensors," *IEEE Trans. Circuits Syst. II, Analog and Digital Signal Processing*, vol.47, no.12, pp.1468–1475, 2000.
- [4] F. Luthon and D. Dragomirescu, "A cellular analog network for MRF-based video motion detection," *IEEE Trans. Circuits Syst. I, Fundamental Theory and Applications*, vol.46, no.2, pp.281–293, 1999.
- [5] H. Yamada, T. Miyashita, M. Ohtani, and H. Yonezu, "An analog MOS circuit inspired by an inner retina for producing signals of moving edges," *IEICE Technical Report*, NC99-112, 2000.
- [6] M. Kawaguchi, T. Jimbo, and M. Umeno, "Motion detection artificial vision model by the two-dimensional analog electronic circuits," *Proc. ICONIP2000*, FBP29, Taejon, Korea, 2001.
- [7] M. Kawaguchi, M. Uno, T. Jimbo, and M. Umeno, "Speed and direction detecting artificial vision model by the two-dimensional analog electronic circuits," *Proc. SNPD'01*, pp.900–907, Nagoya, Japan, 2001.
- [8] M. Kawaguchi, C. Shao, T. Jimbo, and M. Umeno, "Motion detecting two-dimensional three-layers analog electronic circuits using biomedical vision model," *Neural Information Processing*, Fudan University Press, *Proc. ICONIP2001*, pp.1225–1230, Shanghai, China, 2001.
- [9] M. Kawaguchi, T. Jimbo, and M. Umeno, "Motion detection two-dimensional MOS analog electronic circuits using biomedical vision model," *Proc. SCI2001*, vol.6, pp.309–314, Orlando, USA, 2001.



Masashi Kawaguchi received the B.E. degree in Information Engineering from the Nagoya Institute of Technology in 1987. He joined Kaisei High School as a mathematics teacher in 1987. He was transferred Suzuka National College of Technology as a Research Associate in the Department of Electrical Engineering in 1992. He is also now working toward the D.E. degree in Environmental Technology and Urban Planning Graduate School of Engineering at Nagoya Institute of Technology. He is a member of the IEE of Japan and IPSJ (Japan).



Takashi Jimbo received the B.E. and M.E. degrees in electronics and the D.E. degree in electrical engineering from Nagoya University in 1970, 1972, 1978, respectively. He joined Nagoya University as a research associate in 1975. He stayed at the City College of New York, U.S.A. and studied nonlinear optics from 1985 to 1986. He was transferred to Nagoya Institute of Technology in 1987. He was promoted to a professor in 1993 and shifted from the Research Center for Micro-Structure Devices to the Department of Environmental Technology & Urban Planning in 1997. He is studying semiconductor opt-electronics including the development of lasers and solar cells. He is a member of Phys. Soc. Japan, Japan Soc. Appl. Phys., Laser Soc. Japan, Japan Soc. Infrared Sci., Inst. Elect. Eng. Japan, Japan Soc. Medical Electron. Bio. Eng. and Soc. Instru. Control Eng. (Japan).



Masayoshi Umeno graduated from Nagoya Institute of Technology in 1960 and received M.E. degree from Tokyo Institute of Technology in 1962. He became a research associate in 1962, an assistant professor in 1969 at Nagoya Univ. He became a professor at Nagoya Institute of Technology in 1978. From 1990 to 1996, He was a director of Center for Cooperative Research. From 1993 to 1996, he was a director of Research Center for Micro-Structure Devices. From 1996 to 1998 he was a vice president of Nagoya Institute of Technology. He was transferred to Chubu University in 2001. He has studied the interactions of semiconductor photo-devices, especially photon drag photodetectors for semiconductor lasers, photo-transistors, high efficiency solar cells, image sensors, crystal growth of various semiconductors for semiconductor devices. Recently, studying multi-layer thin film crystal growth by MOCVD, heteroepitaxy on Si and their application to optical integrated circuits, 3-dimensional circuits such as artificial retina and parallel processing of image. He won the Yonezawa prize in 1967 and the Award from IEE Japan with the Kodaira Memorial Prize in 1991. Dr. Umeno is a member of Inst. TV Eng. Japan, Soc. Instru. Control Eng. (Japan), Japan Soc. Appl. Phys., Phys. Soc. Japan, and IEEE.